Journal of the Korean Nuclear Society
Volume 35, Number 4, pp.356～368, August, 2003

〈Technical Note〉

Performance Analysis of The KALIMER Breakeven Core Driver Fuel Pin Based on Conceptual Design Parameters

Dong Uk Lee, Byoung Oon Lee, Young Gyun Kim, Ki Bog Lee, and Jin Wook Jang
Korea Atomic Energy Research Institute
150 Dukjin-dong Yuseung-gu, Daejeon 305-353, Korea
dulee@kaeri.re.kr

(Received December 11, 2002)

Abstract

Material properties such as coolant specific heat, film heat transfer coefficient, cladding thermal conductivity, surface diffusion coefficient of the multi-bubble are improved in MACSIS-Mod1. The axial power and flux profile module was also incorporated with irradiation history. The performance and feasibility of the updated driver fuel pin have been analyzed for nominal parameters based on the conceptual design for the KALIMER breakeven core by MACSIS-MOD1 code. The fuel slug centerline temperature takes the maximum at 700mm from the bottom of the slug in spite of the nearly symmetric axial power distribution. The cladding mid-wall and coolant temperatures take the maximum at the top of the pin. Temperature of the fuel slug surface over the entire irradiation life is much lower than the fuel-clad eutectic reaction temperature. The fission gas release of the driver fuel pin at the end of life is predicted to be 68.61% and plenum pressure is too low to cause cladding yielding. The probability that the fuel pin would fail is estimated to be much less than that allowed in the design criteria. The maximum radial deformation of the fuel pin is 1.93%, satisfying the preliminary design criterion (3%) for fuel pin deformation. Therefore the conceptual design parameters of the driver fuel pin for the KALIMER breakeven core are expected to satisfy the preliminary criteria on temperature, fluence limit, deformation limit etc.

Key Words : performance, metallic fuel, KALIMER, cladding deformation, eutectic melting , fission gas release

1. Introduction

Since active study began on metallic fuels for liquid-metal reactors (LMRs) at Argonne National Laboratory (ANL), the potential of metallic fuel has grown a great deal. There are many advantages for passive LMR safety, such as good in-reactor performance and low fabrication-recycle costs with the use of metallic fuels. Also metallic fuel has superior characteristics such as high density and high thermal conductivity that enable various high performance core concepts. The technical problems of metallic fuel have been solved through many test irradiation experiences [1].

The ternary (U-30TRU-10Zr) metallic fuel is being considered as the driver fuel of the KALIMER (Korea Advanced LIquid MEtal Reactor) fast reactor that is under development at KAERI. The concept of using ternary fuel in the fast reactor was first developed at ANL and irradiation tests of fuels of various compositions were performed extensively in the EBR-II research reactor. Design of the KALIMER driver fuel rod is a complex process that involves an integration of a wide range of phenomena such as the physical/chemical phenomena, thermal/ mechanical behavior, irradiation behavior etc due to the high power generation rate by fission in the reactor. The KALIMER driver fuel rod is designed to maintain effective in-reactor performance and integrity and to accommodate swelling by temperature, irradiation, thermal expansion, creep, axial expansion etc. To date, the conceptual design for KALIMER breakeven core has been completed [2]. The performance analysis of fuel rod design based on conceptual design parameters is essential to ensure adequate in-reactor fuel performance and its integrity under irradiation conditions.

The purpose of this paper is to evaluate the integrity of the KALIMER Breakeven core driver fuel pin through performance analysis under irradiation conditions and the feasibility of the nominal design parameters of the pin by updated MACSIS-Mod1 code. Section 2 describes the conceptual design of the KALIMER breakeven core driver fuel pin and section 3 describes the performance requirements of the fuel rod. The updated MACSIS-Mod1 code [3] was used for the performance analysis and its results for the KALIMER breakeven core driver fuel pin are given in section 5. Conclusions are given in the final section.

2. Description on Conceptual Design of KALIMER Driver Fuel Pin

The axial configuration of an LMR fuel pin is quite different from an LWR fuel pin. In the LMR, the zone containing the fissile fuel (which will form the reactor active-core) is only about a third of the pin axial length, whereas the fuel region of an LWR typically represents 80% of the overall pin length. The LMR core is generally about one metre long, while the entire fuel pin is about three meters long. Because of the much higher core height for a similarly powered LWR, overall pin lengths for the LWR and LMR systems are comparable.

The base alloy, ternary (U-TRU-10%Zr) metal fuel is used for the KALIMER breakeven core as the driver fuel. The fuel pin is made of sealed tubing containing fissile and fertile materials in columns. The fuel is immersed in sodium for thermal bonding with the cladding. The fuel cladding material is ferritic-martensitic steel. In LMR fuel rod, a fission gas plenum is located in the pin as a reservoir for gaseous fission products produced during irradiation. The fission gas plenum is normally long, approximately 1～1.5

Table 1. Nominal Design Parameters for KALIMER Driver Fuel Pin

Fuel slug	U-30TRU-10Zr
Fuel slug diameter (mm)	5.46
Fuel slug density (TD, g/cm^3)	17.5
Smeared density (%)	75
Pin P/D ratio	1.203
Pin outer diameter (mm)	7.4
Integrated gap between fuel and clad (mm)	0.84
Pin inner diameter (mm)	6.3
Cladding thickness (mm)	0.55
Pin overall length (mm)	3708.1
Fuel slug length (mm)	1000
Plenum length (mm)	1565
Pin pitch (mm)	8.9
Wire diameter (mm)	1.4

times of the active core height. In general, the plenum can be located either above or below the core. For example, in the early U.S. designs (FFTF and CRBRP), the plenum is above the core. A fission gas plenum at the KALIMER fuel pin is located above the fuel slug and sodium bond. The bottom of the driver fuel pin is a solid rod end plug for axial shielding.

Tag gas capsules are sometimes included in the plenum region to assist the location of a failed fuel pin. These capsules in the fuel pins contain an isotopic blend of inert gases that are unique to that assembly. At the time of final fabrication, the capsule is punctured so that the gas mixture enters the fission gas plenum. Should a break occur in the cladding during irradiation, the unique blend of gases would escape with the fission gases into the primary loop where they could be collected and analyzed to identify the assembly containing the failed pin. In designs employing a wire pin spacing technique, the wire is normally pulled through a hole in each end cap and then welded at that point. For some designs the wire is merely laid along the side of the end cap and then welded. The nominal design parameters for the driver fuel pin of KALIMER breakeven core are shown in Table 1[4].

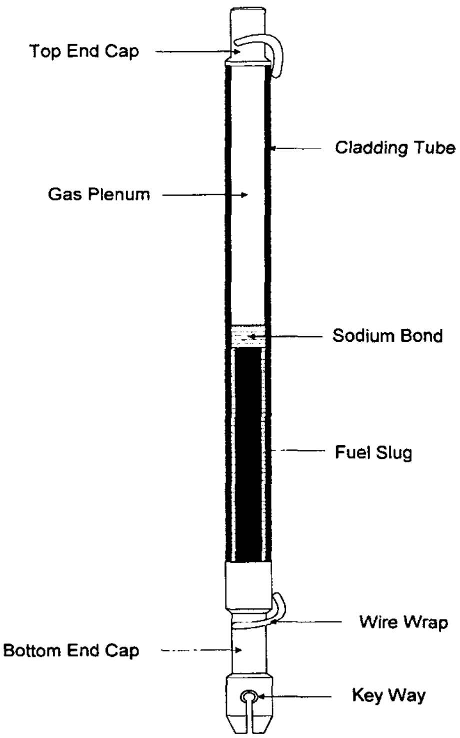

Fig. 1. The Overview of the Fuel Rod Design Used in KALIMER

As shown in Table 1, the overall length of the KALIMER driver fuel pin is 370.8 cm and the outer diameter is 7.4 mm. The pitch is 8.9 mm and pitch to diameter ratio is 1.203. Diameter of fuel slug, cladding thickness, pin inner diameter and gap are 5.46, 0.55, 6.3, 0.84 mm respectively. Figure 1 shows the overview of the fuel rod design used in KALIMER.

3. Performance Requirements

The important performance aspect to be considered in the design of the driver fuel rod for the KALIMER is to maintain the integrity of the fuel element under normal operating conditions. The most important irradiation performance characteristics of metallic fuel element are its diameter increase and FCI (fuel cladding interaction) between fuel slug and clad; resulting from fuel swelling, fission gas release and internal pressure buildup, cladding creep, and the interdiffusion of fuel and cladding constituents. Since the density of ferritic-martensitic cladding does not change significantly as a result of irradiation, the fuel slug volume change shall be considered as one of the major performance parameters.

Fuel rod design is a complex process that involves an integration of a wide range of phenomena. The rod design procedure must integrate the thermal analysis of the pin with an assessment of the characteristics of the fuel and cladding as a function of temperature and irradiation history and with stress analysis of the fuel-cladding system. In actual design practice, all of the governing processes must be integrated in large time-dependent pin analysis computer codes. Design basis requirements shall be satisfied within 2-sigma uncertainty allowances [2].

The important performance aspects to be considered in the designs of the driver fuel are the stabilities of the fuel rod and assembly-duct in the presence of swelling, fission product release behavior, burnup limit, cladding wastage and cladding deformation. The most important irradiation performance characteristic of metallic fuel is the diametral increase of fuel slug resulting from fuel swelling. Since cladding density does not change significantly as a result of irradiation, a lower smeared density of fuel element shall be considered. The following are the performance requirements:

1) Thermal conductivity and maximum fuel temperature; the thermal conductivity of fuel slug shall be sufficiently high so that in-reactor maximum operating temperatures will be easily restricted to less than the melting temperature of the fuel slug.
2) The temperature at interface between fuel slug and cladding inside shall be maintainable to less than 700°C under normal operation condition.
3) The fuel slug materials shall be stable thermo-chemically under irradiation, and shall corrode slowly in event of a clad defect.
4) The diametral increase of fuel element shall be compatible with the thermal-hydraulic requirements, and in any event shall be less than 3%.
5) Cladding wastage during fuel life in-reactor shall be minimal.
6) The integrity of fuel elements shall be maintainable up to 20% local-burnup of the initial material
7) The fuel assembly duct shall be designed to minimize vibrations, which might cause damage to the fuel assembly ducts themselves or to their flow tubes.

4. Description on Updated MACSIS-Mod1 Code

The MACSIS-Mod1 code [5] has been developed for the design analysis of metallic fuel for KALIMER by KAERI. The MACSIS-Mod1 is a computer code that calculates thermal performance characteristics and dimensional changes of the fuel rods in liquid-metal fast reactor. It consists of a series of subroutines that model LMR fuel phenomena. The MACSIS-Mod1 calculates temperature distribution, dimensional changes, fission gas release, and the radial redistribution of the fuel-alloying elements during irradiation in the metallic fuel slug. The fuel rod is divided into a specified number of axial nodes, and then one-dimensional calculations are performed in each axial node.

A detailed thermo-mechanical analysis is performed in the radial direction by dividing the fuel region into ten concentric annuli of equal thickness. In the axial direction, the fuel can be divided into up to 20 nodes, while the plenum is treated as a single node. The operating condition of each node is specified by the linear power and fast flux. The axial nodes are thermally coupled only through the calculated coolant temperatures.

MACSIS-Mod1 consists of a driving routine, input/output routines, mathematical models, and a physically based theoretical model for fission gas release as well as a correlated model for fuel swelling. The mathematical models are heat transfer, gas pressure, and to some extent dimensional change of fuel and cladding. Up to now, the MACSIS-Mod1 has been upgraded by improving sub-models, such as axial power and flux profile with burnup, temperature calculation, fission gas release, and rod deformation. The details of the MACSIS-Mod1 show in Table 2. Figure 2 shows a MACSIS-Mod1 flowchart.

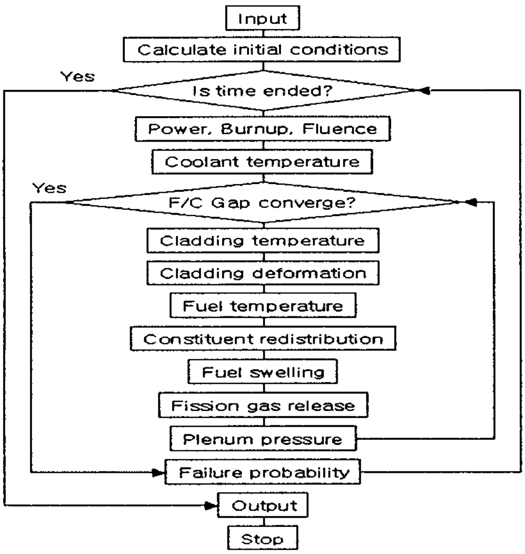

Fig. 2. The Flowchart of MACSIS-MOD1 Code

Fuel temperature

The precise prediction of fuel temperature distribution is one of the most important factors in a fuel performance code. The key factors affecting the temperature distribution of metallic fuel are known to be porosity formation, bond sodium infiltration into the porosity, and the heat generation rate and thermal conductivity dependence on fuel constituent migration. These parameters are incorporated into the fuel temperature calculation schemes of MACSIS-Mod1 as described below.

One-dimensional steady-state heat conduction equation in a cylindrical coordinate is described as,

$$rk(r)\frac{\partial T}{\partial r} + \int_0^r rq'''(r)dr = 0 \qquad (1)$$

where r is the radial position, T is the temperature, k is the thermal conductivity and q''' is the volumetric heat generation rate. The benchmark results for predicted temperature by MACSIS-Mod1 are already presented in reference 3. It is apparent that MACSIS has a reasonably

Table 2. The Details of the Updated MACSIS-Mod1

	Old	Update [15,16,17]
Coolant specific heat	Input value	$C_p = 1630.16 - 0.4629(1.8T+491.67) + 1.4276\times10^{-4}(1.8T+491.67)^2$
Film heat transfer coefficient	Input value	$\frac{k(4.0+0.16(P/D)^5 + 0.33(P/D)^{3.8}(Pe/100)^{0.86})}{De}$
Surface diffusion coefficient	$9.5\times10^{-4}\exp(-43000/RT)$	$7.4\times10^{-2}\exp(-30T_m/RT)$ for $T/T_m > 0.07$ $1.4\times10^{-6}\exp(-13T_m/RT)$ for $T/T_m < 0.07$
Cladding thermal conductivity	$29.65 - 6.668\times10^{-2}T + 2.184\times10^{-4}T^2 - 2.527\times10^{-7}T^5 + 9.621\times10^{-11}T^4$	$17.622+2.428\times10^{-2}T - 1.696\times10^{-5}T^2$ for $T < 1027$ $12.027+1.218\times10^{-2}T$ for $T < 1050$
Axial power & flux profile with burnup	No	Yes

good capability in predicting fuel pin rod temperatures.

Fuel constituent redistribution

The radial fuel constituent migration related to the formation of three distinct phasal zones is a general phenomenon in irradiated U-Pu-Zr and U-Zr alloys. This phenomenon may affect the in-reactor performance of metallic fuel rods, influencing such factors as melting temperature, thermal conductivity, power generation rate, phase boundaries and porosity distribution of the fuel slug. Thus, constituent redistribution modeling is essential when developing a metallic fuel performance code. The redistribution model adopted in MACSIS-Mod1 was basically identical to Hofman's model [14].

Fission gas retention and release

The first step of fission gas release in metal fuel is the movement of fission gas created in the fuel matrix to the fuel grain boundary as well as in oxide fuel. The second step of fission gas release is the movement of fission gas on the grain boundary through the fission gas tunnels to the fuel rod gas plenum. Remaining gases on grain boundary are precipitated into gas bubbles and they have contributed to the fuel swelling due to gas bubble growth. As described in the reference 3, in the intra-granular fission gas release model, the Booth's classical diffusion theory was directly adopted. Multi-bubble size distribution on the grain boundary and the average number of bubbles per unit volume at given i bubble size range, $\bar{f}_i$, is estimated by [3]:

$$\int_{n_i}^{n_{i+1}} F(m\ ,\tau,n)dn = \overline{f}_i(n_{i+1} - n_i)$$

where n_i is number of gas atoms in the i size bubble and τ is reduced time as a dimensionless parameter. The total number of gas atoms arriving at a unit area of the grain boundary m_{gb} must equal the summation of the gas atoms over the multiple-bubble-size distribution. Hence, using $\bar{f}_i$ from the above equation, the following balance equation can be written as follows:

$$m_{gb} = C_s \sum_{size\ range} \overline{f}_i \cdot \frac{(n_i + n_{i+1})}{2}$$

where C_s is the correction coefficient for the concentration per unit area of the grain boundary. Therefore, the real number of bubbles for median atoms size at given bubble size range is given by:

$$f_i = \bar{f}_i \cdot C_s$$

The major part of the gas atoms xenon and krypton are deposited in the matrix. They then diffuse slowly under the combined effects of the temperature and the fission spikes, which continuously perturb the crystal structure. Some of them find a path to the grain boundaries where they coalesce in bubbles. Based on a simple cubic structure in two-dimensions, the critical fraction of the grain-boundary area occupied by bubbles when interlinking first occurs is:

$$\left(\frac{r_{sb}}{R_{sb}}\right)^2_{crit} = \frac{\pi r_{sb}^2}{(2r_{sb})^2} = \frac{\pi}{4}$$

where r_{sb} is the radius of a gas bubble and Rsb is the radius of a circular unit cell of the grain boundary. Therefore, the saturation condition for a unit area of the grain boundary is given by

$$\frac{1}{4} = \sum_{size\ range} (r_{lb,i})^2 \cdot f_i$$

Dimensional changes of the fuel

Fuel deformation is primarily due to retained fission gas bubbles on the grain boundary, and solid fission product accumulation within the matrix including liquid phase products. The sum of the volumes of the bubbles trapped on the grain boundary is determined, and the fractional swelling is calculated. Finally, swelling caused by solid fission products is added to obtain the total fission-induced swelling. These two mechanisms are incorporated into MACSIS-Mod1.

The fuel thermal expansion is computed by finding volumetric average radial displacement. At each radial node, the displacement is computed using the coefficient of thermal expansion given by [3]:

$$\alpha^f = \alpha_0^f + \alpha_T^f \times T \quad (2)$$

where α^f is the coefficient of thermal expansion, cm/cm-℃ and T is the temperature, ℃.

The volumetric average thermal expansion is then computed by :

$$\overline{\Delta D / D} = \int_{r_c}^{r_0} \alpha^f T r dr / [1/2(r_0^2 - r_c^2)] \quad (3)$$

Table 3. Nuclear Performance Summary of Breakeven Core

Average breeding ratio	1.051
Refueling intervals(months)	18
Burnup reactivity swing(pcm)	896
Average driver fuel assembly discharge burnup(MWD/kg)	87.6
Peak driver fuel discharge burnup(MWD/kg)	120.7
Feed driver fuel enrichment(wt.%)	
Total TRU in U-TRU	30.00
Average linear power for driver fuel(W/cm)	
BOL	201.2
EOL	186.2
Peak linear power for driver fuel(W/cm)	287.1
Power peaking factor for driver fuel	
BOL	1.427
EOL	1.448
Peak neutron flux for driver fuel($\times 10^{15}$n/cm^2/s)	3.01
Peak discharge fast fluence for driver fuel($\times 10^{23}$n/cm^2)	2.41

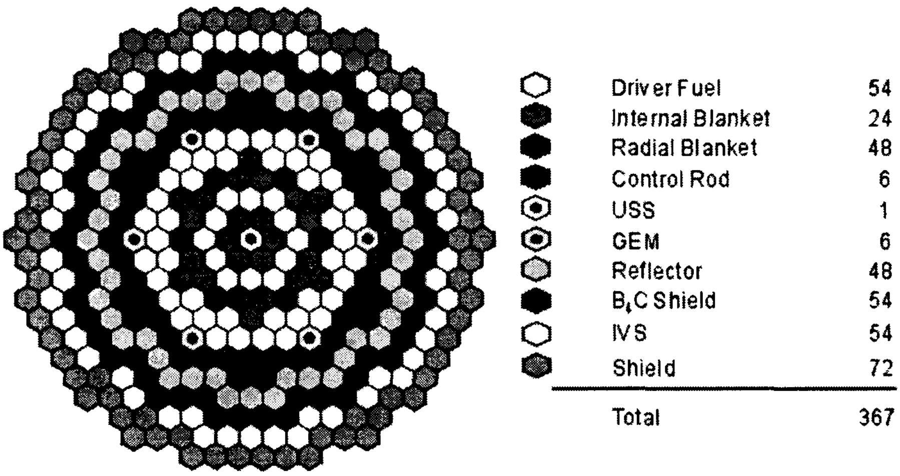

Figure 3. The Overview of KALIMER Breakeven Core

where r_o is the cladding inner surface radius, and r_c is the cladding outer surface radius. The integration in Eq. (3) is performed numerically using the trapezoidal rule.

The fuel radius at operating conditions is then computed using :

$$r'_f = (r_0 + \Delta D_s) \times \left(1. + \overline{\Delta D / D}\right) \quad (4)$$

where r'_f is the "hot" fuel radius, and ΔD_s is the amount of fuel swelling.

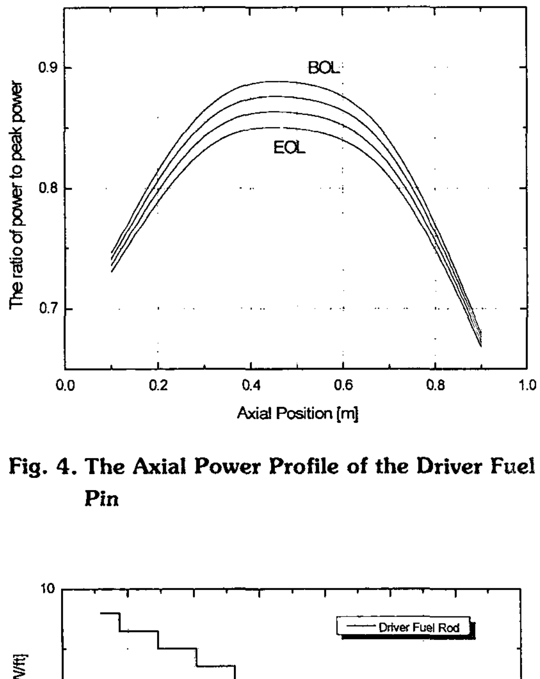

Fig. 4. The Axial Power Profile of the Driver Fuel Pin

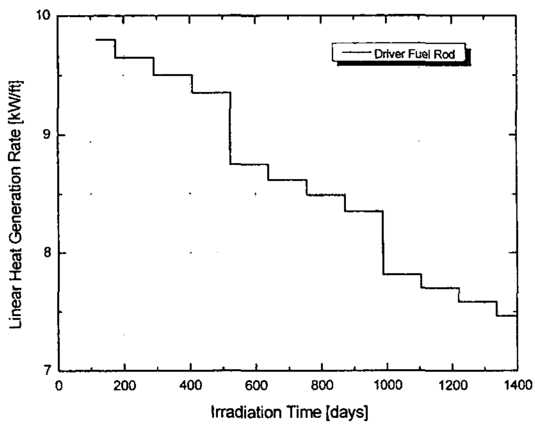

Fig. 5. The Irradiation History of the Driver Fuel Pin

5. Performance Analysis of the Driver Fuel Pin

Performance analysis and feasibility evaluation for conceptual design parameters of the KALIMER breakeven core driver fuel pin are performed based on axial power and flux profile data computed by the KALIMER core design group [2]. According to 1/3 refueling system and 18 months cycle, in order to analyze the most severe fuel pin, the pin is selected in DR0301 assembly, which is located in the first ring of driver assembly as is shown in Figure 3 and generates the highest power. Also the evaluation is performed applying the batch factor (1.2) of the breakeven core to consider three cycles. Figure 4 and 5 show the change of the axial power profile and irradiation history as burnup proceeds and performance summary of the breakeven core is shown in Table 3.

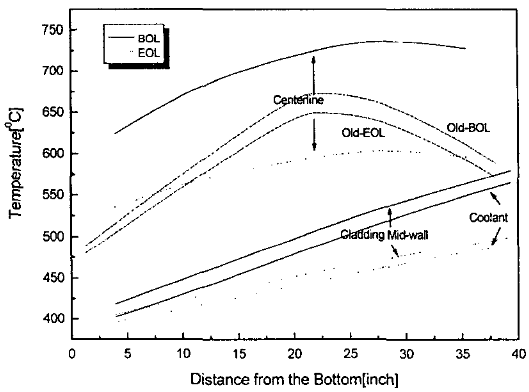

Fig. 6. Axial Distributions of Fuel Slug Center, Cladding Mid-wall and Coolant Temperature

Temperature distribution and behavior prediction

Figure 6 shows the axial distributions of the temperatures of fuel slug centerline, cladding mid-wall and coolant at BOL and EOL. The fuel slug centerline temperature takes the maximum at 700 mm from the bottom of the slug, although the peak of the linear power rate is at the nearly core mid-plane (500 mm from the bottom). This is the result of the tight thermal coupling between the coolant and the slug due to the Na bonding and high thermal conductivity of the slug, while cladding mid-wall and coolant temperatures take the maximum at the top of the pin. The temperature difference between BOL and EOL is based on change of the axial power profile shown in Figure 4.

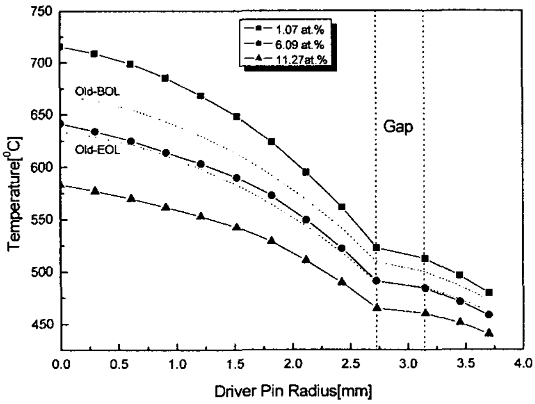

Fig. 7. Radial Temperature Distribution of Driver Fuel Pin

When there is a peak power at the axial midpoint of the driver fuel rod, radial temperature distribution of the fuel rod at that point as burnup proceeds is shown in Figure 7. As is shown in Figure 7, outer surface temperature of the cladding depending on power profile of the pin is about 440-479℃ during the entire irradiation life. While the temperature difference between fuel slug surface and cladding inner surface at BOC (beginning of life) is predicted to be about 9.4℃ by old MACSIS-Mod1, the updated MACSIS-Mod1 predicted to be about 10.6℃ and then generally decreases as burnup increases. As the linear power increases, the temperature difference between outer surface and inner surface of the cladding increases. It appears at about 32.8℃ at BOL and then somewhat decreases after that.

For irradiation temperatures less than 540℃, as in the in-reactor creep data they are consistent with a stress exponent of $1 \leq n < 2$, creep is relatively insensitive to temperature but it gets sensitive to the temperature range higher than 570℃. And for the temperature range higher than 650℃, HT9 alloy no longer displays the in-reactor creep resistance that it exhibited at irradiation temperatures less than 570℃, since the HT9 in-reactor creep increases with a stress exponent of the order 3 to 7[6]. Therefore as the cladding mid-wall temperature of the maximum deformation position at EOL is about 450-496℃ during the entire irradiation life, creep due to the rod internal pressure increase except the extreme pressure almost does not occur. According to the evaluation results, the plenum pressure is about 1091 psi at EOL and gives stress much less than cladding yield stress, 50170 psi. Therefore the cladding deformation due to the stress by plenum pressure slightly occurs.

One of the major interests related to the in-reactor integrity of metallic fuel rod is the fuel-cladding eutectic reaction. For metallic fuel rod using HT9 alloy, the eutectic temperature under the steady state is about 700℃[7]. The position

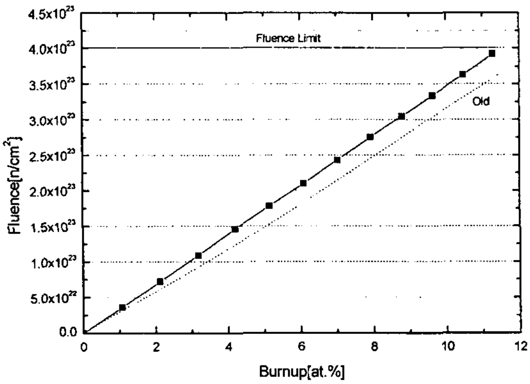

Fig. 8. Fluence of the Driver Fuel Pin

which eutectic reaction occurs is the interface between fuel slug surface and inner surface of the cladding. Therefore it is predicted that the eutectic reaction occurs slightly because the maximum temperature of the fuel slug surface is about 584 ℃.

Fluence and swelling for cladding

Based on ANL irradiation test results, it is reported that swelling of HT9 alloy is negligibly small up to $3.7\times10^{23}n/cm^2$ fluences [8]. However because of no test data for more fluence than $3.7\times10^{23}n/cm^2$, an experiment for limit criteria with fast fluence is required from the point of view of a cladding swelling limit. Based on the evaluation results using the fast peak flux($3.01\times10^{15}n/cm^2/s$) for breakeven core driver fuel pin as shown in Figure 8, axial center position(the 3rd node) located in axial peak fluence achieves $3.98\times10^{23}n/cm^2$ which approaches the irradiation fluence limit at EOL.

The significant factor of the damage due to cladding deformation is an excessive deformation resulted from stress increase by increase of the rod internal pressure under irradiation. As irradiation swelling for HT-9 is getting bigger, the coolant channel becomes smaller but does not lead to cladding damage itself. For driver fuel pin, irradiation swelling of HT9 alloy at EOL is 1.76% and this is a dominant phenomenon affected by the total cladding deformation. However the total pin deformation (1.93%) including this result is less than preliminary design criteria (3%). Therefore it is thought that the integrity of the driver fuel pin during the entire irradiation life is expected to satisfy the preliminary criteria.

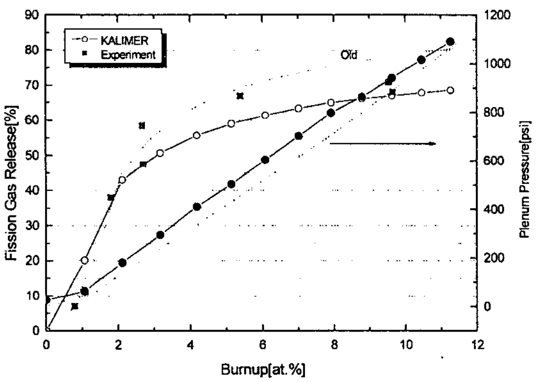

Fig. 9. Fission Gas Release and Plenum Pressure of the Driver Fuel Pin

Fission gas release

The result of fission gas release predicted by updated MACSIS MOD1 are presented for burnup values up to 11.27 at.%. Figure 9 shows the percentage gas release according to burnup variation, predicted by the semi-theoretical models [9] developed by KAERI. According to the experimental results [13], it appears that fission gas release largely increases at around 1 to 2 at.% burnup. The maximum fission gas release predicted at a burnup of 11.27 at.% was 68.61 %. The prediction by MACSIS MOD1 with the semi-theoretical models agrees comparatively well with the experimental results from ANL, according to burnup increase. It seems that the capability of efficiently predicting fission gas release in MACSIS MOD1 was improved. The plenum pressure at EOL is about 1091 psi as is shown in Figure 9 and this result is much less than cladding yield strength, 50170 psi (346MPa at 450 ℃).

CCDF(cladding cumulative damage fraction)

The fuel pin performance also can be predicted using rupture correlation of the fuel pin. The CCDF is determined from time-to-rupture correlation as a function of temperature and stress. The time-to-rupture correlation is usually obtained through the fitting of biaxial tube rupture tests. Generally, the correlation may be expressed in terms of Larson-Miller parameter (LMP), Dorn parameter or other formulas [10]. But present lifetime correlation does not consider hazards of environmental errors and uncertain material behaviors, such as pin vs. pin interaction, pin-duct interaction, hot spots, fretting wear, handling damage, etc. The fuel pin should be designed to maintain its structural integrity during its lifetime under normal operating conditions. CCDF shall not be greater than the following criteria [11];

- Steady state operation: < 0.001
- Transient operation: < 0.2

Figure 10 shows CCDF and hoop stress increase due to plenum pressure as burnup proceeds. The more burnup increases, the more rod internal pressure increases and also hoop stress and CCDF increase. But compared to design criteria under steady state operation, the probability that the fuel pin would fail is small because the CCDF value is much less than the design criteria.

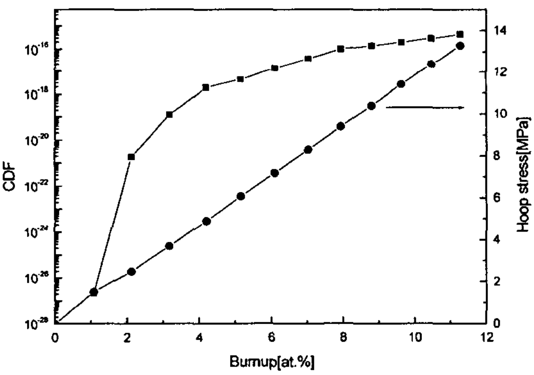

Fig.10. CCDF and Hoop Stress of the Driver Fuel Pin

Pin deformation

As fission gas release of metallic fuel pin under irradiation is high, creep deformation due to rod internal pressure at high burnup is a significant in-reactor behavior parameter. For fuel pin with 75% smeared density, cladding deformation actually observed at high burnup appears smaller and creep due to stress by plenum pressure increase at high burnup and swelling due to irradiation and temperature at low burnup is a major cause of fuel rod deformation [12].

Fuel rod deformation was calculated by MACSIS MOD1 combining all of the models described in reference 3. The peak flux and coolant inlet temperature used for calculation are 3.01×10^{15} n/cm^2 · sec and 386.2℃ respectively. The calculation results indicated that the main factor that causes cladding strains of the ternary/HT9 fuel pin was a swelling under plenum pressure. Figure 11 shows the axial deformation at EOL of the pin. The axial deformation takes the maximum at the second node from the bottom of the pin. Figure 12 shows the comparison of the cladding strains predicted by the updated MACSIS MOD1 code. The total cladding strain at EOL is predicted to be 1.93% and this result is less than the design criteria (3%). The dominant factor affecting the total strain is the irradiation swelling of cladding as is shown in Figure 12. This is the result of the fractional volume change effect due to void formation rather than solid state reactions. Also if cladding mid-wall temperature is more than 400 ℃ in the temperature range that thermal creep is not active, the steady state swelling

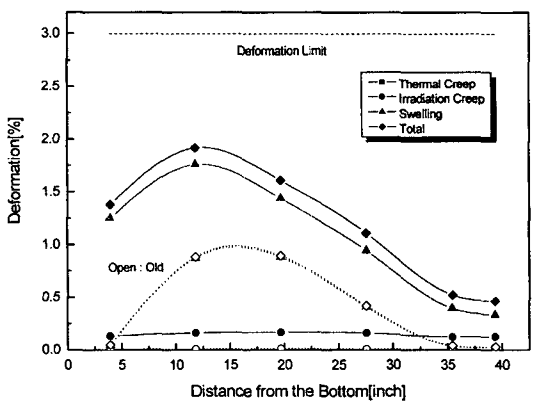

Fig. 11. Axial Deformation at EOL of the Driver Fuel Pin

rate decreases depending on temperature as shown in figure 13. Therefore although cladding mid-wall temperature has a maximum at the top of the slug, strain due to fractional volume change appears near the bottom, since the fractional volume change effect due to void formation is a function of the steady state swelling rate.

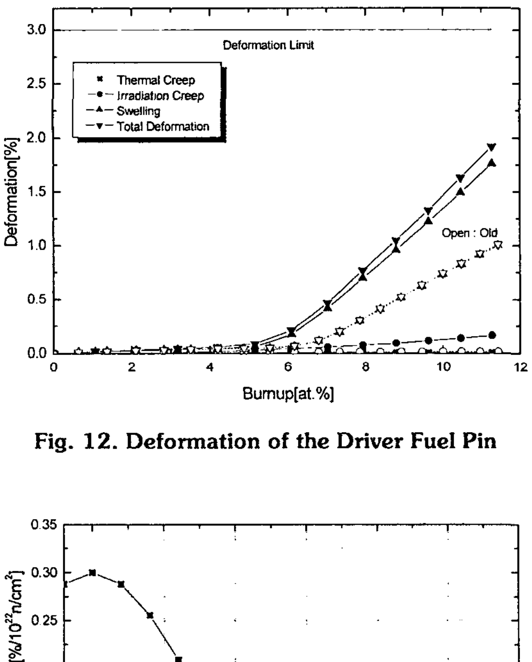

Fig. 12. Deformation of the Driver Fuel Pin

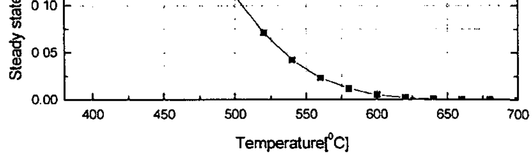

Fig. 13. Steady State Swelling Rate with Temperature of HT9 Alloy

6. Conclusions

In this study, material properties such as coolant specific heat, film heat transfer coefficient, cladding thermal conductivity, surface diffusion coefficient of the multi-bubble are improved in MACSIS-Mod1. The axial power and flux profile module was also incorporated with irradiation history. The performance and feasibility of the driver fuel pin have been analyzed for nominal parameters based on the conceptual design for the KALIMER breakeven core by MACSIS-MOD1 code. The major results are as follows;

- ▶ The fuel slug centerline temperature takes the maximum at 700 mm from the bottom of the slug. The Maximum of fuel slug surface and cladding mid-wall temperature is an axial top of active fuel slug. Temperature of fuel slug surface at that point is much less than eutectic reaction temperature.
- ▶ The maximum fluence of the driver fuel pin at EOL is slightly less than irradiation fluence limit.
- ▶ The fission gas release of the driver fuel pin at EOL is 68.61% and stress by plenum pressure is much less than cladding yield stress. These results show that in-reactor performance and feasibility for design parameters is good.
- ▶ The probability that fuel pin would fail is small because the CCDF value is much less than the criteria.
- ▶ When EFPD(effective full power day) is 1395 days, the burnup achieved of the driver fuel pin is 11.27 at.% and maximum deformation of fuel pin is 1.93%. This result also satisfies design criteria (3%); therefore integrity of the driver fuel pin is expected to satisfy the preliminary criteria.

Finally, the conceptual design parameters of the driver fuel pin for the KALIMER breakeven core satisfy preliminary criteria for design parameters such as eutectic reaction temperature, fluence limit, deformation limit etc. Therefore it is concluded that in-reactor performance and integrity of the driver fuel pin designed at the conceptual design step are expected to satisfy the preliminary criteria. The updated MACSIS-Mod1 code shows that its general potential improvement as a design tool for the performance analysis of a metallic fuel rod is identified.

Acknowledgement

This project has been carried out under the Long-Term R&D Program supported by the Ministry of Science and Technology (MOST) of Korea.

References

1. G.L. Hofman and L.C. Walters, "Metallic Fast Reactor Fuels", *Material Science and Technology,* Volume 10A, Part I, 1994.
2. D.H. Han et. al., "KALIMER Conceptual Design Report", *KAERI/TR-2204/2002*, KAERI, 2002.
3. W. Hwang, B.O. Lee, Y.J. Kim, "Recent Improvements in Modelling Fission Gas Release and Rod deformation on Metallic Fuel in LMR", *Annals of Nuclear Energy*, 00/27, 2000.
4. W. Hwang et. al., "KALIMER Fuel System Preliminary Design Description", *KAERI/TR-1145/98*, KAERI, 1998.
5. W. Hwang et. al., "MACSIS Program User's Manual and Code Description", *KAERI/TR-1531/2000*, KAERI, 2000.
6. R.J. Puigh, "In-Reactor Creep of Selected Ferritic Alloys", *Twelfth International Symposium ASTM STP 870*, 1985.
7. W. Hwang et. al., "Preliminary Evaluation Report on Design Criteria for KALIMER Fuel", KAERI/TR-1216/99, KAERI, 1999.
8. A.L. Pinter et. al., ANS 1993 Winter Meeting, San Francisco, 1993.
9. W. Hwang et. al., "A Comprehensive Fission Gas Release Model Considering Multiple Bubble Sizes on the Grain Boundary Under Steady State Conditions", *Nucl. Tech.*, 95, 314(1991).
10. A.E. Walter and A.B. Reynolds, "Fast Breeder Reactors", Pergamon Press, 1981.
11. W. Hwang et. al., "Guideline for Design Requirement on KALIMER Driver Fuel Assembly Duct", *KAERI/TR-940/98*, KAERI, 1998.
12. G.L. Hofman, L.C. Walters, and T.H. Bauer, "Metallic Fast Reactor Fuels", *Prog. Nucl. Energy*, 31, 83(1997)
13. A.M. Yacout et. al., "Average Irradiation Temperature for the Analysis of In-Pile Integral Measurements", *Nucl. Tech.*, 115, 61(1991).
14. G.L. Hofman, S.L. Hayes, M.C. Petri, "Temperature gradient driven constituent redistribution in U-Zr alloys", *J. Nucl. Mater.*, 227, 277(1996).
15. Y.G. Kim, "The Thermal Hydraulic Data for Breakeven Core Assembly Design", *IOC-CD-002-2001*, Jan. (2001).
16. Sandvik Data Sheet, "SANDVIK HT9", S-1720-ENG, SANDVIK Steel Catalogue, May. (1981).
17. E. Gruber and J.M. Kramer, "Modeling Fission Gas Behavior in Metallic Fuels", *J. Am. Ceram. Soc.* 70[10]699-703, (1987).